Exp. is still running. Official report follows (28.7.99)

Report on preliminary experiments: HS702

T. Baumbach, D. Lubbert, J. Schneck, L. Leprince

The aim of the experiment was the characterisation of the strain behaviour in free-standing *surface gratings* based on periodic multilayers with alternating tensile and compressive strain (zero net strain),

The structures consist of (GaIn)(AsP)/InP superlattices grown by metalorganic vapour phase epitaxy (MOVPE), fabricated by CNET Bagneux, France Telecom. The composition was chosen in such a way that the strain in both sub-layers has the same amount but opposite sign. These symmetrically strained layer superlattices have been laterally patterned in [1 10]-direction by lithography and subsequent etching providing surface gratings with typical periods of 250 nm.

The idea of the experiment was the investigation of the multilayer surface gratings in symmetrical, asymmetrical and grazing incidence diffraction geometry, in order to be sensitive to the vertical and the lateral component of the inhomogeneous strain field.

A triple crystal diffractometer set-up was used. The experiments were performed at a wavelength of 0.8 A in order to reach high-order reflections (660 and 668), which are particularly sensitive to the lattice strain,

GID is depth selective and allows moreover to measure independently the influence of the grating shape and the lateral strain component by recording reciprocal space maps around the complementary [HHO]- and [H-HOI-reciprocal lattice points (RLPs).

Asymmetrical diffraction (around the RLPs [HHL]) is additionally sensitive to the *vertical* strain component. Moreover, the contributions from the different materials are separated in vertical (q_z-) direction in this geometry.

In order to evaluate the experimental data, we compared them with calculations of the strain field in the sample based on elasticity theory and carried out with the help of a Finite Element Method. From these data, reciprocal space maps could be simulated and quantitatively compared to the experimental results (see fig. 4 and 5).

Fig. 1: measured map of the [668]-| reflection in asymmetric scattering geometry. We observe well-resolved grating truncation rods, proving the macroscopically homogeneous grating periodicity. Each truncation rod contains vertical satellite peaks, which represent the superlattice periodicity. The strong peak in the middle stems from the substrate material; it is surrounded by an intense cloud of diffuse scattering. The groups of peaks below and above it correspond to the two different materials that form the multilayer. For both of them, the maximum of the envelope of the peaks is shifted to the left with respect to the substrate, i.e. towards larger lateral lattice constants. This shift indicates a slight lattice strain relaxation of one layer, which gives rise to additional strain in the other one. One reason for this behaviour is a rest non-zero net strain in the averaged superlattice with respect to the substrate.

Fig. 2: measured map of the [6-60]- reflection in grazing incidence geometry. This diffraction geometry allows to investigate the form of the surface grating separately from the influence of strain. Besides the Yoneda peaks characteristic for low angles of incidence ($\alpha_i=\alpha_c$),| the map shows the upper half of a cross pattern, indicating an approximately trapezoidal form of the grating.

Fig. 3: measured map of the [660]-| reflection in grazing incidence geometry.

Apart from the influence of strain, the scattering geometry at this reflection is similar to that of fig.2. All the relevant differences in the two maps must therefore be caused by the strain field.

Fig. 4: Simulated reciprocal space map at the [668]- reflection (to be compared with fig. 1). Apart from the diffuse cloud (which we did not try to simulate), all the relevant features are reproduced: lateral grating truncation rods and vertical satellites, substrate- and two layer-peaks, shift of the envelope to the left.

Fig. 5: Distribution of the lateral component ε_{xx} of the strain field in the sample, as calculated by a Finite Element Method. The simulation in fig. 4 is based on these data

Fig.1

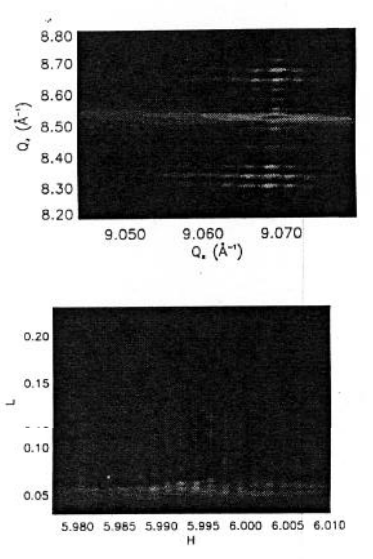

Fig. 3

Fig.2

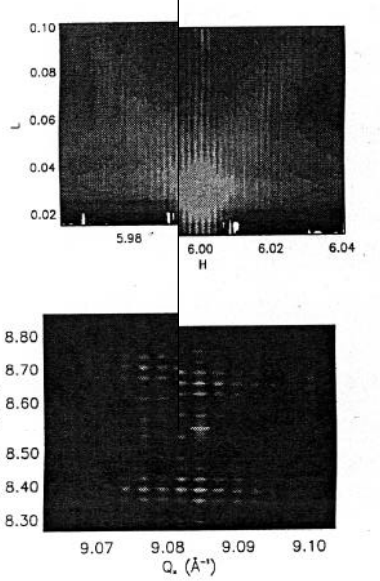

Fig.4

Fig.5